Journal of Engineering Mathematics **35:** 199–217, 1999.

Ringing loads on a slender vertical cylinder of general cross-section

O. M. FALTINSEN
Department of Marine Hydrodynamics, Norwegian University of Science and Technology, Trondheim, Norway.
e-mail: oddfall@marin.ntnu.no

Received 5 May 1997; accepted in revised form 26 March 1998

Abstract. Third harmonic loads on a vertical cylinder in irregular or regular longcrested waves in deep water are analyzed. Characteristic wave lengths are large relative to the cross-dimensions of the cylinder. Characteristic wave amplitudes are of the same order as the cylinder cross-dimensions. The method is a generalization of the FNV method (Faltinsen, Newman and Vinje [1]) for a circular cross-section. Integral theorems and auxiliary potentials are used to simplify the force expressions. Details are shown for Lewis form sections. Completely analytical expressions are derived for elliptical cross-sections. It is demonstrated that the third harmonic loads are sensitive to the cross-sectional form.

Keywords: hydrodynamics, offshore structures, nonlinear wave loads, potential flow, hydroelasticity

1. Introduction

Ringing is of concern in survival conditions for gravity-based structures (GBS) and tension-leg platforms (TLP) in deep water. Ringing is caused by extreme waves exciting transient resonance response of structural modes. The relevant resonance periods are significantly lower than the peak period T_p of the wave spectrum. The interesting natural periods for a TLP and GBS are about one fourth and one third of T_p, respectively. This means that third and fourth harmonic load terms are needed in the analysis.

A TLP is restrained from oscillating vertically by tethers, which are vertical anchorlines that are tensioned by the platform buoyancy being larger than the platform. The submerged part of the platform may consist of four vertical columns penetrating the free surface. Horizontal pontoons connect the columns at the lower end of the column. The draught of the platform may be around 40 m. The cross-sections of the columns of a TLP are normally circular. The diameter D may be from 20 to 30 m. The Draugen monotower is an example of a GBS. It has non-circular cross-sections that vary along the cylinder axis. It is installed on 252·5 water depth. The smallest cross-dimension of the tower is 15 m and close to the free surface. The ringing analysis has to be performed in an irregular sea. A typical wave period and maximum wave amplitude A for survival conditions in the North Sea could be 15 m and 15 s. The wave number K for linear harmonic plane waves with period 15 s is 0·01789 m^{-1}. It means that representative values of KD and A/D are 0·35 and 0·75 with $D = 20$ m.

Basic studies on ringing loads on a fixed vertical and infinitely long circular cylinder in deep water incident waves were reported by Faltinsen, Newman and Vinje [1] (FNV) and by Newman [2]. FNV assumed regular incident waves and Newman considered irregular waves. Their procedure will be generalized to a monotower with non-circular cross-sections varying along the cylinder axis. The cross-section has two symmetry axes. The waves are longcrested

and propagating along one of the symmetry axes. The incident waves are characterized by a wave amplitude A of the same order of magnitude as a characteristic cross-dimensional length a of the structure. Both a and A are $O(\varepsilon)$, where $\varepsilon \ll 1$. The characteristic wave length is $O(1)$. The presented theory includes load terms of $O(A^3)$. First, second and third harmonic load terms are included. The theory can be generalized to other wave headings, cross-sections without symmetry planes and a multicolumn GBS. The effect of body motion can be included. Generalization of the method for a TLP needs further study. The effects of junctions between columns and pontoons, heave forces and roll and pitch moments should be evaluated. Both wave frequency and slowdrift motions of a TLP need to be included. The present theory gives fourth-order harmonic terms in roll and pitch moments about an axis close to the mean free surface. The reason is that the third harmonic loads act in the free surface zone with a center of action that follows the incident wave elevation in time. But all fourth-order harmonic terms are not consistently included in the analysis.

Rainey [3] has analysed a similar case that we study. An important difference in the present analysis is a nonlinear scattering potential ψ arising from the free-surface conditions. If we disregard the effect of ψ, then there is a difference in how Rainey and we derive the loads. Our formulas are derived by direct pressure integration and use of integral theorems. Rainey uses conservation of momentum and energy in the fluid.

The solution of ψ implies satisfaction of an inhomogeneous free-surface condition, three-dimensional Laplace equation and a homogeneous body-boundary condition for the normal derivative of ψ. The free-surface condition is satisfied on a horizontal plane following the linear incident wave elevation ζ_{I1} at the cylinder axis. FNV solved this problem by Weber transform for a circular cylinder. High numerical accuracy is needed if a direct numerical method is used. This is demonstrated by Zhu [4] for a circular cylinder. The problem of solving for ψ is avoided in this paper. Integral theorems are instead used to rewrite the forces due to ψ. This simplifies the analysis. Details are shown for cross-sections that can be described by Lewis-form technique and conformal mapping. Completely analytical expressions are derived for elliptical cross-sections. Numerical results are presented and show that the third-harmonic loads are sensitive to the cross-sectional form.

Malenica and Molin [5] have presented a theory for third-harmonic loads on a vertical circular cylinder in incident regular waves. It is valid for any wave length relative to the cylinder radius and based on a conventional perturbation scheme of the free-surface conditions about the mean water level. Third-order terms are included. They discard the steady second-order potential and the third-order potential oscillating with the frequency ω of the linear loads. The second-order potential oscillating with 2ω and the third-order potential oscillating with 3ω are consistently included according to their perturbation analysis.

Since the nonlinear scattering potential ψ varies rapidly in the vertical direction over distances on the scale of the incident wave amplitude, it is not possible in our analysis to use a conventional perturbation of the free-surface conditions about the mean water level. The free-surface condition for ψ is satisfied on a horizontal plane following ζ_{I1}. Since the assumptions in the presented theory and the theory by Malenica and Molin [5] are different, they need not give the same results. However, Malenica and Molin demonstrated that their results agreed with FNV for very long wave lengths relative to the cylinder radius. The amplitude of the third-harmonic loads, but not the phases, agrees reasonably in the wave-length domain of interest for ringing analysis of a GBS or a TLP.

Experiments have revealed the existence of highly nonlinear local flow phenomena close to a vertical circular cylinder when the column is being ‘hit’ by a large and steep wave. The wave

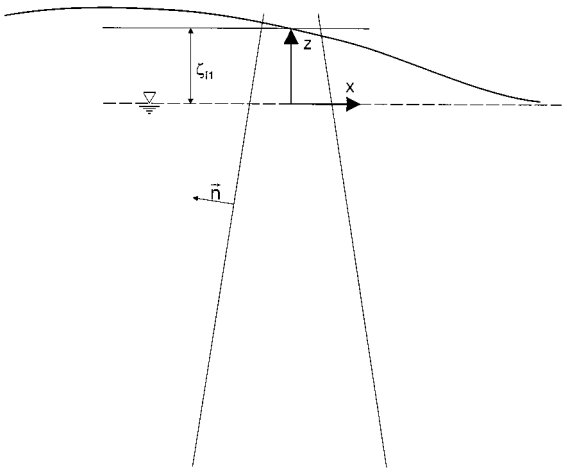

Figure 1. Description of vertical cylinder and coordinate system. Incident linear wave system is illustrated.

length is large relative to the diameter and the wave amplitude is of the order of the cylinder radius. The nonlinear flow near the column may be characterized as a so called 'hydraulic jump' starting on the upstream side of the column at the time instant when there is a wave trough at the column axes. A hydraulic jump is propagating on each side of the column and collide on the downstream side. The consequence of the collision between the two hydraulic jumps is a strong vertical jet flow (run-up) which can hit the platform deck. The phenomenon is most pronounced in regular incident waves. The time between the formation and collision of the hydraulic jumps is half the wave period. There are no pronounced 'hydraulic jumps' propagating upstream in the half-wave period after the collision. The present theory does not predict phenomena like this. It is of both academic and practical interest to study this problem in the future.

The paper is organized as follows. The theory for a general cross-section is first presented. Details are then shown for Lewis forms and elliptic sections. The following chapter on numerical results gives the complete third-harmonic horizontal load expressions for a vertical cylinder with either a Lewis-form section or an elliptic section.

2. Theory

Cartesian coordinates (x, y, z) are defined with $z = 0$ in the mean water level (see Figure 1). Positive z is upwards. The x-y planes and y-z planes are symmetry planes for the cross-section of the monotower. The surface normal vector $\vec{n} = (n_1, n_2, n_3)$ is positive into the fluid domain. Incident longcrested irregular or regular waves propagating along the x-axis are studied. The characteristic wave amplitude A and structural cross-dimension a are $O(\varepsilon)$, where $\varepsilon \ll 1$. The characteristic wave length is $O(1)$. The cylinder (monotower) is slender and fixed. The cross-sectional shape can vary slowly along the cylinder length so that $n_3 = O(\varepsilon)$. Potential flow is assumed. The total velocity potential is written as $\phi = \phi_I + \phi_S + \psi$, where ϕ_I is the incident wave potential. ϕ_s is the first-order scattered potential and ψ represents higher-order nonlinear scattering. The exact boundary-value problem is that ϕ satisfies a three-dimensional Laplace equation, the body boundary condition $\partial\phi/\partial n = 0$ and the free-surface condition

$$\phi_{tt} + g\phi_z = -2\nabla\phi \cdot \nabla\phi_t - \tfrac{1}{2}\nabla\phi \cdot \nabla(\nabla\phi)^2, \quad \text{on } z = \zeta \tag{1}$$

outside the body. Here g is the acceleration of gravity, t is the time variable and ζ is the water elevation. Initial conditions are needed with this formulation of the free-surface condition. The boundary-value problem will be simplified similar as FNV did. Deep water is assumed. The linear incident-wave system is described by a superposition of plane harmonic waves. If harmonic incident waves of frequency ω and wave number K are considered, then the linear waves are correct to order $(KA)^3$ if the dispersion relation is written as $\omega^2/g = K(1+(KA)^2)$, (*cf.* Newman [6, Eq. (6.39)]). In irregular sea there is a second-order velocity potential that oscillates with difference frequencies $\omega_i - \omega_j$, for any pair of frequencies ω_i and ω_j of the spectral components of the linear wave system (*cf.* Faltinsen [7, pp. 169]). It follows then from the free-surface conditions that the third-order terms in the incident wave system will have no sum-frequency components $\omega_i + \omega_j + \omega_k$, where ω_i, ω_j and ω_k are three spectral components of the linear wave system (Newman [2]).

The function ϕ_S can be found by slender-body theory and matched asymptotic expansions. We can write $\phi_D = \phi_I + \phi_S$ to first order in A as

$$\phi_D = \phi_{I0} + u(x + \phi_{11}) + u_x(\tfrac{1}{2}x^2 + \phi_{21}) + w\phi_{25} + f(z,t) + O(\varepsilon^4) \tag{2}$$

in the near field of the cylinder. Here ϕ_{I0}, u, u_x, w are functions of z and time t and the values of ϕ_I, $\partial\phi_I/\partial x$, $\partial^2\phi_I/\partial x^2$, $\partial\phi_I/\partial z$ at $x = 0$, $y = 0$. The incident-wave potential has been expanded in a Taylor series about $x = 0$, $y = 0$ in Equation (2). ϕ_{11}, ϕ_{21} and ϕ_{25} satisfy a 2-D Laplace equation in the cross-sectional plane and the body-boundary conditions.

$$\frac{\partial\phi_{11}}{\partial N} = -n_1, \qquad \frac{\partial\phi_{21}}{\partial N} = -xn_1, \qquad \frac{\partial\phi_{25}}{\partial N} = -n_3. \tag{3}$$

Here $\vec{N} = (n_1, n_2)$. ϕ_{11} has a 2-D dipole behavior far away from the cylinder and matches with a far-field 3-D horizontal dipole distribution along the cylinder axis; ϕ_{25} and part of ϕ_{21} have a far-field source-like behavior; $f(z,t)$ is a consequence of matching with a far-field 3-D source distribution along the cylinder axis. This matching is similar as for a slender body in infinite fluid (*cf.* Newman [6], Ch. 7). It follows from the boundary-value problem that $\phi_{11} = O(\varepsilon)$, $\phi_{21} = O(\varepsilon^2)$, $\phi_{25} = O(\varepsilon^2)$, $f(z,t) = O(\varepsilon^3)$. It is shown later in the text that the three-dimensional hydrodynamic interaction potential $f(z,t)$ does not cause any horizontal forces to $O(\varepsilon^5)$.

Further, ψ is a consequence of that ϕ_s does not satisfy the free-surface condition to correct order of magnitude. As noted in the introduction, the variation of ψ along the cylinder length is the same order of magnitude as the variation in x and y. So ψ satisfies a 3-D Laplace equation. The principal free-surface condition for the nonlinear potential is

$$\psi_{tt} + g\psi_z = -2\nabla\phi\cdot\nabla\phi_t - \tfrac{1}{2}\nabla\phi\cdot\nabla(\nabla\phi)^2 \quad \text{on } z = \zeta. \tag{4}$$

On the right side of Equation (4) the term $-(u^2 + w^2)_t$ is neglected because it is associated with the nonlinear effects on the incident-wave potential. This term is included in the analysis of the incident-wave potential. Equation (4) can be approximated. The term ψ_{tt} is of higher order than $g\psi_z$. Due to the strong z-variations of ψ it is essential that the formulation of the free-surface condition for ψ is based on perturbations about the linear incident free-surface elevations and not about $z = 0$. The free-surface condition is

$$g\frac{\partial\psi}{\partial z} = -2uu_t\left(2\frac{\partial\phi_{11}}{\partial x} + (\nabla\phi_{11})^2\right)$$

$$-\tfrac{1}{2}u^3\left(2\frac{\partial^2\phi_{11}}{\partial x^2}+2\frac{\partial}{\partial x}(\nabla\phi_{11})^2+\nabla\phi_{11}\cdot\nabla(\nabla\phi_{11})^2\right) \tag{5}$$

on $z=\zeta_{I1}$ (FNV). ζ_{I1} is the linear incident free-surface elevation at $x=0$, $y=0$. The body-boundary condition is $\partial\psi/\partial n=0$; ψ will be asymptotically small when $(z-\zeta_{I1})=O(\varepsilon)$. It follows from (5) that $\psi=O(\varepsilon^3)$.

The horizontal loads per unit length due to ϕ_I and ϕ_s only can be written as

$$F'=\rho_w A_c(z)\frac{\mathrm{D}u}{\mathrm{D}t}+a_{11}(z)\frac{\partial u}{\partial t}+w\frac{\partial}{\partial z}(ua_{11}(z))+O(\varepsilon^5) \tag{6}$$

for a totally wetted cross-section. Here $A_c(z)=$ cross-sectional area, $\rho_w=$ mass density of the fluid, $\mathrm{D}/\mathrm{D}t$ is the substantial derivative and

$$a_{11}=\int_\Sigma \phi_{11}n_1\,\mathrm{d}s$$

is the two-dimensional added mass for translatory motion in the x-direction; Σ is the cross-sectional surface curve. Equation (6) can be found by starting out with Bernoulli's equation for the pressure p, *i.e.*

$$\begin{aligned}p/\rho_w \;=\; & -gz-\left[\frac{\partial\phi_I}{\partial t}+\tfrac{1}{2}|\nabla\phi_I|^2\right]-\frac{\partial\phi_s}{\partial t}-\frac{\partial\phi_I}{\partial x}\frac{\partial\phi_s}{\partial x}\\ & -\frac{1}{2}\left[\left(\frac{\partial\phi_s}{\partial x}\right)^2+\left(\frac{\partial\phi_s}{\partial y}\right)^2\right]-\frac{\partial\phi_I}{\partial x}\frac{\partial\phi_s}{\partial z}-\frac{1}{2}\left(\frac{\partial\phi_s}{\partial z}\right)^2.\end{aligned} \tag{7}$$

Terms of $O(\varepsilon^2)$ will be included in the pressure. The last term can then be neglected. The hydrostatic pressure term $-\rho_w gz$ will be analyzed later. The pressure in the incident waves $-\rho_w[\partial\phi_I/\partial t+\frac{1}{2}|\nabla\phi_I|^2]$ gives the first term in Equation (6). This follows from the divergence theorem applied on the volume inside the body. The second term follows from the $-\rho_w\partial\phi_s/\partial t$-term and from the fact that ϕ_{21}, ϕ_{25} and $f(z,t)$ will not contribute to the force. We can derive the last term by first noting that

$$\frac{1}{2}\int_\Sigma n_1(\nabla\phi_s)^2\,\mathrm{d}s=\int_\Sigma\left(\frac{\partial\phi_s}{\partial n}\right)\left(\frac{\partial\phi_s}{\partial x}\right)\mathrm{d}s.$$

This is a consequence of

$$\begin{aligned}&-\int_\Sigma\vec{n}\cdot\left[\frac{\partial\phi_s}{\partial x}\nabla\phi_s-\vec{i}\frac{1}{2}\left(\left(\frac{\partial\phi_s}{\partial x}\right)^2+\left(\frac{\partial\phi_s}{\partial y}\right)^2\right)\right]\mathrm{d}s\\ &\quad=\iint_{\mathrm{vol}}\nabla\cdot\left[\frac{\partial\phi_s}{\partial x}\nabla\phi_s-\vec{i}\frac{1}{2}\left(\left(\frac{\partial\phi_s}{\partial x}\right)^2+\left(\frac{\partial\phi_s}{\partial y}\right)^2\right)\right]\mathrm{d}\tau=0.\end{aligned}$$

We have here used the divergence theorem on the two-dimensional volume Vol between the body surface Σ and a circular control surface Σ_∞ far away from the body and the facts that the surface integral over Σ_∞ is zero and that the integrand of the volume integral is zero.

By using the body boundary conditions we obtain

$$\tfrac{1}{2}\rho_w \int n_1 \left(\left(\frac{\partial \phi_s}{\partial x} \right)^2 + \left(\frac{\partial \phi_s}{\partial y} \right)^2 \right) \mathrm{d}s$$

$$= \rho_w \int_\Sigma \frac{\partial \phi_s}{\partial n} \frac{\partial \phi_s}{\partial x} \mathrm{d}s = -\rho_w \int_\Sigma \frac{\partial \phi_I}{\partial x} \frac{\partial \phi_s}{\partial x} n_1 \mathrm{d}s - \rho_w w \int_\Sigma \frac{\partial \phi_s}{\partial x} n_3 \, \mathrm{d}s.$$

The first term on the right-hand side cancels the force due to the pressure term $-\rho(\partial\phi_I/\partial x)(\partial\phi_s/\partial x)$ in Equation (7). This means that the pressure terms

$$-\rho_w \frac{\partial \phi_I}{\partial x} \frac{\partial \phi_s}{\partial x} - \tfrac{1}{2}\rho_w \left[\left(\frac{\partial \phi_s}{\partial x} \right)^2 + \left(\frac{\partial \phi_s}{\partial y} \right)^2 \right] - \rho_w \frac{\partial \phi_I}{\partial z} \frac{\partial \phi_s}{\partial z}$$

in Equation (7) causes the following horizontal force over a segment of $\mathrm{d}z$

$$\rho_w w \iint \left[\frac{\partial}{\partial z}(u\phi_{11}) n_1 - \frac{\partial}{\partial x}(u\phi_{11}) n_3 \right] \mathrm{d}S.$$

The function ϕ_s is here approximated as $u\phi_{11}$. The next steps are to use Stokes theorem and divide the force with $\mathrm{d}z$. The result is the last term in Equation (6).

The integration of the total pressure force which acts on the cylinder in the x-direction can be decomposed into integrations from $z = -\infty$ to $z = 0$, from $z = 0$ to $z = \zeta_{I1}$ and from $z = \zeta_{I1}$ to $z = \zeta_{I1} + \zeta_2$. Here $\zeta_{I1} + \zeta_2$ is the local wave elevation at the cylinder surface correct to $O(\varepsilon^2)$. It includes both the effect of the incident waves and the locally scattered free surface. The contribution by integration of (6) from $z = 0$ to $z = \zeta_{I1}$ is

$$F'\zeta_{I1} + \tfrac{1}{2}\zeta_{I1}^2 \frac{\partial^2 u}{\partial t \partial z}(\rho_w A_c + a_{11}) + O(\varepsilon^6). \tag{8}$$

The vertical pressure gradient from $z = \zeta_{I1}$ to $z = \zeta_{I1} + \zeta_2$ is approximately hydrostatic. This means the pressure $p = -\rho g(z - \zeta) + O(\varepsilon^3)$, where ζ is the free-surface elevation. The resulting horizontal force correct to $O(\varepsilon^5)$ is

$$F_{HS} = -\tfrac{1}{2}\rho_w g \int_{\Sigma_1} n_1 \zeta_2^2 \, \mathrm{d}s$$

$$= \rho_w u_t \int_{\Sigma_1} n_1 (x + \phi_{11}) \left[\zeta_{I2} - (u^2/g) \left(\tfrac{1}{2}(\nabla\phi_{11})^2 + \frac{\partial \phi_{11}}{\partial x} \right) \right] \mathrm{d}s, \tag{9}$$

where Σ_1 is Σ at $z = \zeta_{I1}$; ζ_{I2} is the second-order part of the incident wave elevation at $x = 0$, $y = 0$. It can be expressed as

$$\zeta_{I2} = -\frac{1}{g}[\tfrac{1}{2}(u^2 + w^2) - \zeta_{I1} w_t + \partial\phi_{2I0}/\partial t],$$

where ϕ_{2I0} is the second-order incident-wave potential at $x = 0$, $y = 0$, $z = 0$.

The horizontal force due to ψ can be written as

$$F^{(\psi)} = \rho_w \iint_{S_B} \psi_t n_1 \, \mathrm{d}S + \rho_w \iint_{S_B} \nabla\phi_d \cdot \nabla\psi n_1 \, \mathrm{d}S + O(\varepsilon^6). \tag{10}$$

The body surface S_B extends from $z = -\infty$ to $z = \zeta_{I1}$. Solution of ψ involves satisfaction of 3-D Laplace equation, the free-surface condition (5) and the body-boundary condition $\partial\psi/\partial n = 0$. This can be done by Weber transform for a circular cross-section (FNV). If a general cross-section is used, a direct numerical method like a boundary-element method has to be used. It was demonstrated by Zhu [4] for a circular cross-section that a higher-order boundary-element method is needed to get sufficient accuracy. However, it is possible to rewrite Equation (10) so that it is not necessary to solve for ψ. The resulting expressions are much simpler to evaluate. Equation (10) can be rewritten by Green's second identity. We introduce ϕ_{11} as an auxiliary function together with ψ in Green's second identity. Since ϕ_{11} satisfies $\partial\phi_{11}/\partial n = n_1$ on S_B and $\partial\phi_{11}/\partial z = 0$ on S_F, ψ satisfies $\partial\psi/\partial n = 0$ on S_B and there are no contributions from the integrals over a control surface far away from the body, it follows that

$$\iint_{S_B} \psi_t n_1 \,\mathrm{d}s = \iint_{S_F} \phi_{11}\psi_{tz} \,\mathrm{d}s.$$

Here S_F is the horizontal plane outside the cross-section at $z = \zeta_{I1}$. Equation (5) and symmetry and antisymmetry properties of ϕ_{11} and its derivatives give

$$\rho_w \iint_{S_B} \psi_t n_1 \,\mathrm{d}S$$
$$= -(3/g)u^2 u_t \rho_w \iint_{S_F} \mathrm{d}S\, \phi_{11}\left[\frac{\partial^2\phi_{11}}{\partial x^2} + \frac{\partial}{\partial x}((\nabla\phi_{11})^2) + \tfrac{1}{2}\nabla\phi_{11}\cdot\nabla((\nabla\phi_{11})^2\right]. \qquad (11)$$

We reformulate the expressions by the generalized Gauss theorem so that lower-order derivatives occur. This gives

$$\iint_{S_F}\left[\phi_{11}\left(\frac{\partial^2\phi_{11}}{\partial x^2}\right) + \frac{\partial}{\partial x}((\nabla\phi_{11})^2)\right]\mathrm{d}S$$
$$= -\int_{\Sigma_1} n_1\phi_{11}\left[\frac{\partial\phi_{11}}{\partial x} + (\nabla\phi_{11})^2\right]\mathrm{d}s - \iint_{S_F}\left[\left(\frac{\partial\phi_{11}}{\partial x}\right)^2 + \frac{\partial\phi_{11}}{\partial x}(\nabla\phi_{11})^2\right]\mathrm{d}S$$

and

$$\iint_{S_F} \phi_{11}\nabla\phi_{11}\cdot\nabla(\nabla\phi_{11})^2\,\mathrm{d}S$$
$$= -\int_{\Sigma_1}\left(n_1\frac{\partial\phi_{11}}{\partial x} + n_2\frac{\partial\phi_{11}}{\partial y}\right)\phi_{11}(\nabla\phi_{11})^2\,\mathrm{d}s$$
$$-\iint_{S_F}\left(\frac{\partial}{\partial x}\left(\phi_{11}\frac{\partial\phi_{11}}{\partial x}\right) + \frac{\partial}{\partial y}\left(\phi_{11}\frac{\partial\phi_{11}}{\partial y}\right)\right)(\nabla\phi_{11})^2\,\mathrm{d}S.$$

We can simplify this equation by using the body-boundary condition for ϕ_{11} in the integrand of the Σ_1-integral and that ϕ_{11} satisfies the two-dimensional Laplace equation in the integrand of the S_F-integral. Equation (11) can then be written

$$\rho_w \iint_{S_B} \psi_t n_1 \,\mathrm{d}s$$

$$= (3/g)u^2 u_t \rho_w \left\{ \oint_{\Sigma_1} n_1 \phi_{11} \left[\frac{\partial \phi_{11}}{\partial x} + \tfrac{1}{2}|\nabla \phi_{11}|^2 \right] \mathrm{d}s \right.$$

$$\left. + \iint_{S_F} \left[\left(\frac{\partial \phi_{11}}{\partial x} \right)^2 + \left(\frac{\partial \phi_{11}}{\partial x} \right) |\nabla \phi_{11}|^2 + \tfrac{1}{2}|\nabla \phi_1|^2 |\nabla \phi_{11}|^2 \right] \right\} \mathrm{d}S. \tag{12}$$

The second part of Equation (10) can be rewritten as

$$\iint_{S_B} \nabla \phi_D \cdot \nabla \psi n_1 \, \mathrm{d}S = -u \iint_{S_B} \psi \frac{\partial}{\partial s} \left(\frac{\partial}{\partial s}(x + \phi_{11}) \right) \mathrm{d}S.$$

by partial integration. Here $\partial/\partial s$ is the tangential derivative along the body surface in the cross-sectional plane. We introduce an auxiliary potential ϕ_a that satisfies 2-D Laplace equation in x and y and the body-boundary condition

$$\frac{\partial \phi_a}{\partial N} = \frac{\partial}{\partial s} \left(n_1 \frac{\partial}{\partial s}(x + \phi_{11}) \right). \tag{13}$$

By using

(1) Green's second identity with ψ and ϕ_a,
(2) that there are no contributions from the integrals over a control surface far away from the body,
(3) ψ satisfies $\partial \psi / \partial n = 0$ on S_B,
(4) ϕ_a satisfies Equation (13),
(5) $\partial \phi_a / \partial z = 0$ on S_F,
(6) the free-surface condition for ψ and
(7) symmetry and antisymmetry properties of the integrand,

we may derive

$$\rho_w \iint_{S_B} \nabla \phi_D \cdot \nabla \psi n_1 \, \mathrm{d}S = -(2/g)u^2 u_t \rho_w \iint_{S_F} \phi_a \left(2 \frac{\partial \phi_{11}}{\partial x} + |\nabla \phi_{11}|^2 \right) \mathrm{d}S. \tag{14}$$

$F^{(\psi)}$ can be interpreted as a load moving with $z = \zeta_{I1}(t)$ and acting close to $z = \zeta_{I1}(t)$. Only 2-D potentials are needed in the calculations.

2.1. Forces expressed by Lewis-form technique

It will be shown how to evaluate ϕ_{11} and its derivatives, the added mass a_{11}, the auxiliary potential ϕ_a and the integrals given in Equations (9), (12) and (14). The derivation is based on conformal mapping and Lewis-form technique. Since analytical expressions can be extensively used, a good control of numerical accuracy is achieved.

The cross-section is mapped into a circular section of unit radius (see Figure 2). The complex coordinates in the physical and mapped plane are z and ζ, respectively. It is possible to write (see Figure 2)

$$z = x + iy = -ir\, \mathrm{e}^{i\beta}, \tag{15}$$

$$\zeta = \xi + i\eta = -i\rho\, \mathrm{e}^{i\theta}. \tag{16}$$

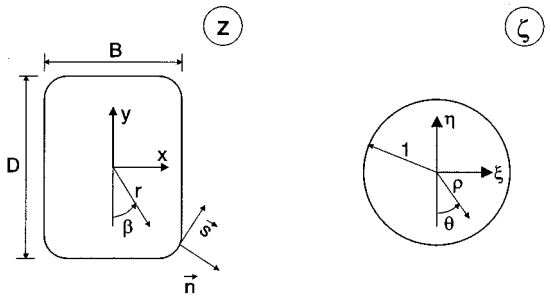

Figure 2. Mapping of a cross-section into a circular section with unit radius.

Here i is the complex unit. The mapping based on Lewis-form technique can be written

$$z(\zeta) = a\left(\zeta + \frac{a_1}{\zeta} + \frac{a_3}{\zeta^3}\right). \tag{17}$$

It can be shown that

$$\begin{aligned} aa_1 &= \frac{1}{2}\left(\frac{B}{2} - \frac{D}{2}\right), \\ aa_3 &= -\frac{1}{4}\left(\frac{B}{2} + \frac{D}{2}\right) + \frac{1}{4}\sqrt{\left(\frac{B}{2} + \frac{D}{2}\right)^2 - 8\left(\frac{A_c}{\pi} - \frac{B}{2}\frac{D}{2}\right)}, \\ a &= \frac{1}{2}\left(\frac{B}{2} + \frac{D}{2}\right) - aa_3, \end{aligned} \tag{18}$$

where B is the cross-sectional dimension in the x-direction at $y = 0$, D is the cross-sectional length in the y-direction at $x = 0$ and A_c is the cross-sectional area. Lewis-form technique is used in ship hydrodynamics to describe submerged cross-sections of ships. The limitations of Lewis-form technique are described by von Kerczek and Tuck [8]. It can be shown that the minimum sectional area coefficient $\sigma = A_c/BD$ for a realistic ship section to exist is $3\pi(2 - B/D)/32$ for $B/D \leqslant 1$ and $3\pi(2 - D/B)/32$ for $B/D \geqslant 1$. The maximum sectional-area coefficient is $\pi(B/D + D/B + 10)/32$. The latter value is always larger than 1. If σ is less than the minimum value, then re-entry forms occur. If σ is larger than the maximum value, then sections with double-valued coordinates as a function of θ occur.

Equation (17) together with Equations (16) and (17) can be written

$$\begin{aligned} x &= a\left[\rho\sin\theta + \frac{a_1}{\rho}\sin\theta - \frac{a_3}{\rho^3}\sin 3\theta\right], \\ y &= -a\left[\rho\cos\theta - \frac{a_1}{\rho}\cos\theta + \frac{a_3}{\rho^3}\cos 3\theta\right]. \end{aligned} \tag{19}$$

The body-boundary condition for ϕ_{11} is

$$\frac{\partial\phi_{11}}{\partial n} = -n_1 \equiv -\frac{\partial y}{\partial s}. \tag{20}$$

The stream function ψ_{11} is introduced. It follows by Cauchy-Riemann's equations that

$$\psi_{11} = -y = a(1-a_1)\cos\theta + aa_3\cos 3\theta \tag{21}$$

on the body boundary. The solution of ψ_{11} in the fluid domain is

$$\psi_{11} = a(1-a_1)\frac{\cos\theta}{\rho} + aa_3\frac{\cos 3\theta}{\rho^3}. \tag{22}$$

This ensures that the flow disappears at infinity. The complex potential can then be written

$$w = \phi_{11} + i\psi_{11} = i\left[\frac{a(11-a_1)}{i\zeta} + \frac{aa_3}{(i\zeta)^3}\right]. \tag{23}$$

The two-dimensional added mass a_{11} can be expressed as

$$\begin{aligned} a_{11} &= \rho_w \int_\Sigma \phi_{11} n_1 \,\mathrm{d}s \\ &= \rho_w \int_0^{2\pi} [a(1-a_1)\sin\theta + aa_3\sin 3\theta][a(1-a_1)\sin\theta + 3aa_3\sin 3\theta]\,\mathrm{d}\theta \\ &= \rho_w \pi (a^2(1-a_1)^2 + 3(aa_3)^2). \end{aligned} \tag{24}$$

We need to evaluate the fluid velocities in Equations (9), (12–14). The complex velocity is

$$\frac{\mathrm{d}w}{\mathrm{d}z} = \frac{\partial\phi_{11}}{\partial x} - i\frac{\partial\phi_{11}}{\partial y} = \frac{\mathrm{d}w}{\mathrm{d}\zeta}\frac{\mathrm{d}\zeta}{\mathrm{d}z},$$

where

$$\frac{\mathrm{d}w}{\mathrm{d}\zeta} = -\left(\frac{a(1-a_1)}{\zeta^2} - \frac{3aa_3}{\zeta^4}\right) \quad \text{and} \quad \frac{\mathrm{d}z}{\mathrm{d}\zeta} = \left(a - \frac{aa_1}{\zeta^2} - \frac{3aa_3}{\zeta^4}\right).$$

This means

$$\begin{aligned} \frac{\partial\phi_{11}}{\partial x} &= \frac{-a^2}{\left|\frac{\mathrm{d}z}{\mathrm{d}\zeta}\right|^2}\left\{\frac{a_1-1}{\rho^2}\cos 2\theta - \frac{(1-a_1)a_1}{\rho^4}\right. \\ &\qquad \left. -\frac{3a_3}{\rho^4}\cos 4\theta - \frac{3a_3}{\rho^6}(1-2a_1)\cos 2\theta + \frac{9a_3^2}{\rho^8}\right\}, \end{aligned} \tag{25}$$

where

$$\left|\frac{\mathrm{d}z}{\mathrm{d}\zeta}\right|^2 = a^2\left\{1 + \frac{a_1^2}{\rho^4} + \frac{9a_3^2}{\rho^8} + \frac{2a_1}{\rho^2}\cos 2\theta - \frac{6a_3}{\rho^4}\cos 4\theta - \frac{6a_1a_3}{\rho^6}\cos 2\theta\right\}. \tag{26}$$

Further we can write

$$\left(\frac{\partial\phi_{11}}{\partial x}\right)^2 + \left(\frac{\partial\phi_{11}}{\partial y}\right)^2 = \frac{a^2}{\left|\frac{\mathrm{d}z}{\mathrm{d}\zeta}\right|^2}\left\{\frac{(1-a_1)^2}{\rho^4} + \frac{6a_3(1-a_1)\cos 2\theta}{\rho^6} + \frac{9a_3^2}{\rho^8}\right\}. \tag{27}$$

We find the auxiliary potential ϕ_a by first introducing the stream function ψ_a. The Cauchy-Riemann equation and Equation (13) give

$$\psi_a = n_1 \frac{\partial}{\partial s}(x + \phi_{11})$$

on the body boundary. We can express this as

$$\psi_a = \frac{[(1 - a_1 + 2a_3)\sin 2\theta + 3a_3 \sin 4\theta]}{[1 + a_1^2 + 9a_3^2 + (2a_1 - 6a_3 a_1)\cos 2\theta - 6a_3 \cos 4\theta]} \tag{28}$$

by using Equations (19–20), (23) and that $\mathrm{d}s^2 = \mathrm{d}x^2 + \mathrm{d}y^2$.

Equation (28) can be written as the Fourier series

$$\psi_a = \sum_{m=1}^{\infty} b_{2m} \sin 2m\theta, \tag{29}$$

where

$$b_{2m} = \frac{1}{\pi} \int_0^{2\pi} \psi_a \sin 2m\theta \, \mathrm{d}\theta. \tag{30}$$

The solution ψ_a can then be written

$$\psi_a = \sum_{m=1}^{\infty} \frac{b_{2m}}{\rho^{2m}} \sin 2m\theta, \tag{31}$$

which means that

$$\phi_a = -\sum_{m=1}^{\infty} \frac{b_{2m}}{\rho^{2m}} \cos 2m\theta. \tag{32}$$

The solution for a circular cylinder is $\phi_a = -\cos 2\theta/\rho^2$.

It will now be shown how to evaluate the different integrals in Equation (12). The first integral can be written

$$\begin{aligned} &\int_{\Sigma_1} n_1 \phi_{11} \left(\frac{\partial \phi_{11}}{\partial x} + \tfrac{1}{2} |\nabla \phi_{11}|^2 \right) \mathrm{d}s \\ &\quad = \int_0^{2\pi} a(\sin\theta(1 - a_1) + 3a_3 \sin 3\theta) \\ &\qquad \times \phi_{11} \left[\frac{\partial \phi_{11}}{\partial x} + \frac{1}{2} \left(\left(\frac{\partial \phi_{11}}{\partial x} \right)^2 + \left(\frac{\partial \phi_{11}}{\partial y} \right)^2 \right) \right] \mathrm{d}\theta, \end{aligned} \tag{33}$$

where

$$\phi_{11} = a[(1 - a_1)\sin\theta + a_3 \sin 3\theta]. \tag{34}$$

The derivatives of ϕ_{11} are given by Equations (26) and (27) with $\rho = 1$. Equation (33) will in general be integrated numerically. However, it will be evaluated analytically for elliptical cross-sections in the next chapter.

We will rewrite the integral over S_F by using ρ and θ as integration variables. This means

$$\mathrm{d}S = \left|\frac{\mathrm{d}z}{\mathrm{d}\zeta}\right|^2 \rho \,\mathrm{d}\rho \,\mathrm{d}\theta. \tag{35}$$

The integration in the ρ-direction will in general be done numerically from $\rho = 1$ to a large number ρ_L and analytically from $\rho = \rho_L$ to ∞. We can write

$$\iint_{S_F} \left(\frac{\partial\phi_{11}}{\partial x}\right)^2 \mathrm{d}S = \int_0^{2\pi} \mathrm{d}\theta \int_1^{\rho_L} \mathrm{d}\rho\, \rho \left|\frac{\mathrm{d}z}{\mathrm{d}\zeta}\right|^2 \left(\frac{\partial\phi_{11}}{\partial x}\right)^2 + a^2\pi\frac{(a_1-1)^2}{2\rho_L^2} + O\left(\frac{1}{\rho_I^6}\right), \tag{36}$$

where $|\mathrm{d}z/\mathrm{d}\zeta|^2$ and $\partial\phi_{11}/\partial x$ are given by Equations (26) and (25). Further

$$\begin{aligned}\iint_{S_F} &\left[\frac{\partial\phi_{11}}{\partial x}|\nabla\phi_{11}|^2 + \tfrac{1}{2}|\nabla\phi_{11}|^2|\nabla\phi_{11}|^2\right]\mathrm{d}S \\ &= \int_0^{2\pi}\mathrm{d}\theta\int_1^{\rho_L}\mathrm{d}\rho\,\rho\left|\frac{\mathrm{d}z}{\mathrm{d}\zeta}\right|^2\left[\frac{\partial\phi_{11}}{\partial x} + \frac{1}{2}\left[\left(\frac{\partial\phi_{11}}{\partial x}\right)^2 + \left(\frac{\partial\phi_{11}}{\partial y}\right)^2\right]\right] \\ &\quad\times\left[\left(\frac{\partial\phi_{11}}{\partial x}\right)^2 + \left(\frac{\partial\phi_{11}}{\partial y}\right)^2\right] + O\left(\frac{1}{\rho_L^6}\right),\end{aligned} \tag{37}$$

where $|\nabla\phi_{11}|^2$ is given by Equation (27).

The integral given by Equation (14) can be expressed analytically as

$$\iint_{S_r} \phi_a\left(2\frac{\partial\phi_{11}}{\partial x} + |\nabla\phi_{11}|^2\right)\mathrm{d}S = \pi a^2(b_2(a_1 - 1 + a_1a_3) - b_4a_3) \tag{38}$$

by the use of the Equations (35), (27), (25) and (32) . Further, b_2 and b_4 are given by Equations (30) and (28).

To sum up, we have shown how to calculate the force component $F^{(\psi)}$ given by Equation (10). This is first split into the two parts given by Equations (12) and (14). Equation (12) is calculated by (36) and (37). Equation (14) is found by (38).

The force component F_{HS} given by (9) can be written

$$F_{HS} = u_t\zeta_{I2}(\rho_w A_c + a_{11}) - (\rho_w/g)u^2u_t\int_{\Sigma_1} n_1(x+\phi_{11})\left(\tfrac{1}{2}(\nabla\phi_{11})^2 + \frac{\partial\phi_{11}}{\partial x}\right)\mathrm{d}s, \tag{39}$$

where the last integral can be calculated similarly as Equation (33). A difference is that (39) involves the factor $x + \phi_{11}$, while (33) has the factor ϕ_{11}; x can be calculated by (16) with $\rho = 1$.

There is in addition a force component given by (8) and the load distribution below $z = 0$ given by (6).

2.2. Forces on elliptic cross-sections

It is possible to express analytically the forces on elliptical cross-sections. Elliptical sections imply that $a_3 = 0$ in (17). This is consistent with

$$A_c = \tfrac{1}{4}\pi BD. \tag{40}$$

Further

$$a = \tfrac{1}{4}(B + D) \tag{41}$$

and

$$a_1 = (B - D)/(B + D). \tag{42}$$

It follows from Equation (24) that

$$a_{11} = \tfrac{1}{4}\rho_w \pi D^2. \tag{43}$$

It is assumed that B is different from zero in the following analysis. It follows from (30) that $b_2 = (1 - a_1)$. Equation (38) can then be written

$$\iint_{S_F} \phi_a \left(2\frac{\partial \phi_{11}}{\partial x} + |\nabla \phi_{11}|^2\right) \mathrm{d}S = -\pi a^2 (1 - a_1)^2. \tag{44}$$

Equation (33) can be written

$$\begin{aligned}\int_{\Sigma_1} n_1 \phi_{11} \left(\frac{\partial \phi_{11}}{\partial x} + \tfrac{1}{2}|\nabla \phi_{11}|^2\right) \mathrm{d}S \\ = a^2(1 - a_1)^2 \int_0^{2\pi} \frac{\sin^2\theta}{1 + a_1^2 + 2a_1 \cos 2\theta} \\ \times [(1 - a_1)\cos 2\theta + (1 - a_1)a_1 + \tfrac{1}{2}(1 - a_1)^2]\,\mathrm{d}\theta = 0.\end{aligned} \tag{45}$$

Similarly we get in (39) that

$$\int_{\Sigma_1} n_1 (x + \phi_{11}) \left(\tfrac{1}{2}|\nabla \phi_{11}|^2 + \frac{\partial \phi_{11}}{\partial x}\right) \mathrm{d}S = 0. \tag{46}$$

We now study the θ-integration in Equation (36) and find that

$$\begin{aligned}\int_0^{2\pi} \left|\frac{\mathrm{d}z}{\mathrm{d}\zeta}\right|^2 \left(\frac{\partial \phi_{11}}{\partial x}\right)^2 \mathrm{d}\theta \\ = a^2 \int_0^{2\pi} \frac{(\cos^2 2\theta + 2b\cos 2\theta + b^2)}{1 + b^2 + 2b\cos 2\theta} \cdot \frac{(a_1 - 1)^2}{\rho^4}\,\mathrm{d}\theta = \frac{(a_1 - 1)^2}{\rho^4}\pi a^2.\end{aligned}$$

Here $b = a_1/\rho^2$. This means that Equation (36) can be written

$$\iint_{S_F} \left(\frac{\partial \phi_{11}}{\partial x}\right)^2 \mathrm{d}S = \frac{\pi}{2}(a_1 - 1)^2 a^2. \tag{47}$$

We now study the θ-integration in (37), i.e.

$$\int_0^{2\pi} \left|\frac{\mathrm{d}z}{\mathrm{d}\zeta}\right|^2 \left[\frac{\partial\phi_{11}}{\partial x} + \frac{1}{2}\left[\left(\frac{\partial\phi_{11}}{\partial x}\right)^2 + \left(\frac{\partial\phi_{11}}{\partial y}\right)^2\right]\right]\left[\left(\frac{\partial\phi_{11}}{\partial x}\right)^2 + \left(\frac{\partial\phi_{11}}{\partial y}\right)^2\right]\mathrm{d}\theta$$

$$= \frac{a^2(1-a_1)^3}{\rho^6}\int_0^{2\pi} \frac{[\cos 2\theta + b + 0.5(1-a_1)/\rho^2]}{1+b^2+2b\cos 2\theta}\mathrm{d}\theta = \frac{a^2(1-a_1)^4\pi}{\rho^4(\rho^4-a_1^2)}.$$

By now integrating in the ρ-direction it follows

$$\iint_{S_F}\left[\frac{\partial\phi_{11}}{\partial x} + \tfrac{1}{2}|\nabla\phi_{11}|^2\right]|\nabla\phi_{11}|^2\mathrm{d}S = \pi(1-a_1)^4\frac{a^2}{4a_1^3}\left[\log\frac{1+a_1}{1-a_1} - 2a_1\right] \tag{48}$$

The limit of this expression when $a_1 \to 0$ *i.e.* for a circle, is $\frac{1}{6}\pi a^2$.

3. Numerical results

The horizontal force part oscillating with frequency 3ω in regular waves will be studied first. This force acts in the free surface. Deep water and a vertical cylinder with constant cross-section are considered. By writing the linear velocity potential for the incident waves as

$$\Phi_I = \frac{gA}{\omega}\,\mathrm{e}^{Kz}\cos(\omega t - Kx),$$

we obtain

$$\zeta_{I1}^2 u_{tz} = \tfrac{1}{4}gK^2A^3(\cos\omega t - \cos 3\omega t),$$

$$wu_z\zeta_{I1} = \tfrac{1}{4}gK^2A^3(\cos\omega t - \cos 3\omega t),$$

$$\zeta_{I2}u_t = -\tfrac{1}{4}gK^2A^3(\cos\omega t + \cos 3\omega t),$$

$$u^2u_t/g = \tfrac{1}{4}gK^2A^3(\cos\omega t - \cos 3\omega t).$$

Here A means the incident wave amplitude and K is the wave number.

Equation (8) gives the following third harmonic load

$$-\tfrac{1}{4}gK^2A^3(a_{11} + \tfrac{1}{2}(\rho_w A_c + a_{11}))\cos 3\omega t. \tag{49}$$

The contribution from (9) or (39) is

$$-\tfrac{1}{4}gK^2A^3\{\rho_w A_c + a_{11} - D_1\}\cos 3\omega t, \tag{50}$$

where

$$D_1 = \rho_w\int_{\Sigma_1} n_1(x+\phi_{11})\left(\tfrac{1}{2}|\nabla\phi_{11}|^2 + \frac{\partial\phi_{11}}{\partial x}\right)\mathrm{d}s. \tag{51}$$

Equation (10) or Equations (12) and (13) give the force contribution

$$-\tfrac{1}{4}gK^2A^3(D_2 + D_3)\cos 3\omega t, \tag{52}$$

where

$$D_2 = 3\rho_w \left[\oint_{\Sigma_1} n_1 \phi_{11} \left(\frac{\partial \phi_{11}}{\partial x} + \tfrac{1}{2} |\nabla \phi_{11}|^2 \right) \mathrm{d}s \right.$$
$$\left. + \int\int_{S_F} \left(\left(\frac{\partial \phi_{11}}{\partial x} \right)^2 + \frac{\partial \phi_{11}}{\partial x} |\nabla \phi_{11}|^2 + \tfrac{1}{2} |\nabla \phi_{11}|^2 |\nabla \phi_{11}|^2 \right) \mathrm{d}S \right] \tag{53}$$

and

$$D_3 = -2\rho_w \int\int_{S_F} \phi_a \left(\frac{\partial \phi_{11}}{\partial x} + |\nabla \phi_{11}|^2 \right) \mathrm{d}S. \tag{54}$$

It is shown in the chapter on Lewis-form technique how D_i can be evaluated.

The sum $F^{3\omega} \cos 3\omega t$ of these force components can be non-dimensionalized as follows:

$$\frac{F^{3\omega}}{\rho_w g K^2 D^2 A^3} \cos 3\omega t. \tag{55}$$

Equation (55) can according to FNV be written as

$$-\frac{\pi}{2} \cos 3\omega t \tag{56}$$

for a circular cross-section. It follows from (40)–(47) that

$$\frac{F^{3\omega}}{\rho_w g K^2 D^2 A^3} = -\frac{\pi}{16} \left\{ 6 + \frac{3}{2} \frac{B}{D} + 3 \frac{D^2 (B + D)}{(B - D)^3} \left(\log \left(\frac{B}{D} \right) - 2 \frac{B - D}{B + D} \right) \right\} \tag{57}$$

for an elliptical cross-section. When $B \to D$, the limit of (57) agrees with (56). Equation (57) is logarithmically singular when $B/D \to 0$, *i.e.* for a flat plate in cross-flow. A potential-flow solution would then in any case be doubtful. Flow separation from the sharp corners should be accounted for in the analysis.

Figure 3 shows non-dimensionalized values of $F^{3\omega}$ as a function of A_c/BD for different values of B/D. The minimum values of A/BD for a realistic cross-section to exist are 0·52, 0·44, 0·29, 0·44 and 0·49 for $B/D = 0{\cdot}25, 0{\cdot}5, 1{\cdot}0, 2{\cdot}0$ and $3{\cdot}0$, respectively. Results for A_c/BD between 0·5 and 1·0 are presented except for $B/D = 0{\cdot}25$ where the lowest value of A_c/BD is 0·55. The results in Figure 3 agree with (57) for an elliptical cross-section. The results for elliptical cross-sections are shown in Figure 4 as a function of B/D. Figure 3 shows that the cross-sectional form clearly influences the magnitude of the force. The highest force amplitudes shown in Figure 3 for $B/D = 1, 2$ and 3 are when $A_C/BD = 1$, while the highest values for $B/D = 0{\cdot}25$ and 0·5 occur for the smallest examined values of A_c/BD. When $B = D$, the minimum force amplitude is not for a circular cross-section, but for A_c/BD between 0·65 and 0·7. What these sections look like can be found from (19) with $\rho = 1$ and a, a_1 and a_3 given by (18). The results in Figure 4 show that the lowest amplitude of the force oscillating with 3ω occur when B/D is between 0·5 and 0·6 for elliptical cross-sections.

The sign of $F^{3\omega}$ is negative for all cross-sections. The meaning of this can be related to the time dependence of the linear horizontal force and the incident wave field. The linear horizontal force is proportional to $\cos \omega t$ and the linear incident-wave field can be described

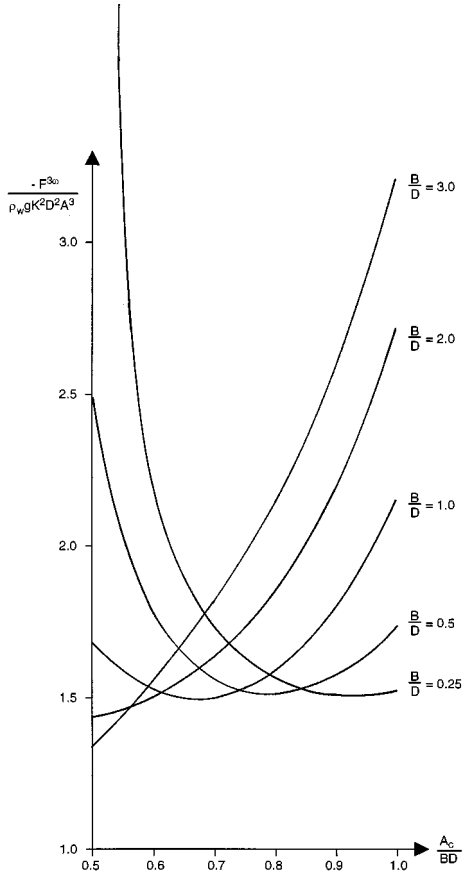

Figure 3. Horizontal force $F^{3\omega}\cos 3\omega t$ acting on a vertical cylinder in incident regular waves propagating in the x-direction on deep water. Cross-section is a Lewis form. K = wave number, A = wave amplitude of incident waves. D = cross-sectional length in the y-direction. B = cross-sectional length in the x-direction. A_C = cross-sectional area.

as $A\sin(\omega t - Kx)$. When the linear horizontal force is a maximum, *i.e.* when there is a wave node at $x = 0$ and the wave slope has a negative minimum, the third harmonic force has a minimum value. When the linear horizontal force has a negative minimum, *i.e.* when there is a wave node at $x = 0$ and the wave slope is a maximum, the third harmonic force has a maximum value. If we consider the time interval from $\omega t = 0$ to π, then $\omega t = 0$ and $\omega t = \pi$ correspond to time instances when the linear horizontal force attains its maximum and negative minimum values, respectively. The third harmonic force has not only $\omega t = 0$ and $\omega t = \pi$ as, respectively, (negative) minimum and maximum values in this time interval. When $\omega t = \pi/3$, the third harmonic force has also a maximum value. This is ahead in time of a maximum incident linear wave elevation at $x = 0$. The wave slope is negative at $x = 0$ at this time instant. The rate of change with time of the incident linear wave elevation is positive. When $\omega t = 2\pi/3$, the third harmonic force has another negative minimum value. This occurs after the time instance when the incident wave has a maximum elevation at $x = 0$. The incident linear wave slope at $x = 0$ is positive and the rate of change with time of the incident linear elevation at $x = 0$ is negative.

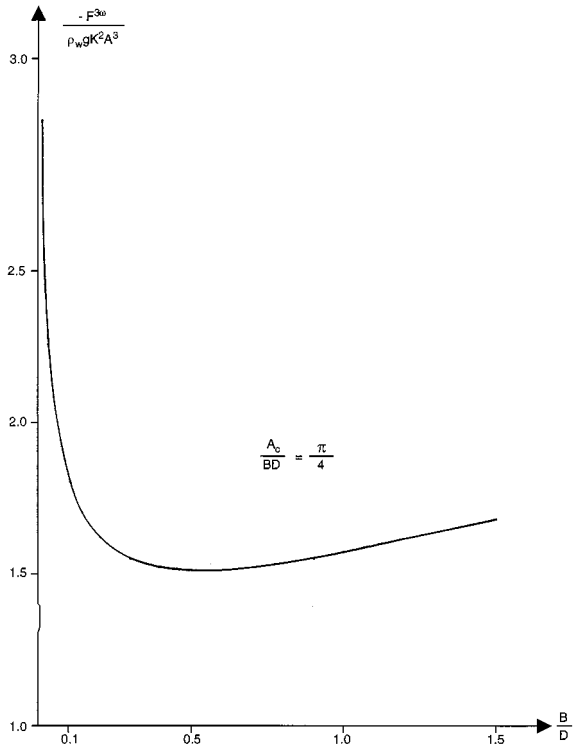

Figure 4. Horizontal force $F^{3\omega}\cos 3\omega t$ acting on a vertical cylinder in incident regular waves propagating in the x-direction on deep water. Cross-section is elliptical. K = wave number, A = wave amplitude of incident waves. D = cross-sectional length in the y-direction. B = cross-sectional length in the x-direction. A_c = cross-sectional area.

The horizontal force expression containing the 3ω-effect in irregular longcrested waves propagating in the positive x-direction can be expressed as

$$F_{irr}^{3\omega} = a_{11}wu\zeta_{I1} + \tfrac{1}{2}(\rho_w A_c + a_{11})\zeta_{I1}^2 u_{tz} + (\rho_w A_c + a_{11})u_t\zeta_{I2} + (-D_1 + D_2 + D_3)u^2u_t/g, \tag{58}$$

where the D_i are defined by (51)–(53). By the 3ω-effect we mean that the expression contains sumfrequency components $\omega_i + \omega_j + \omega_k$, where ω_i, ω_j and ω_k are three spectral components of the linear incident wave system.

For an elliptical cross-section Equation (58) can be written as

$$F_{irr}^{3\omega} = \rho_w\frac{\pi}{4}D^2wu\zeta_{I1} + \tfrac{1}{2}\rho_w\frac{\pi}{4}(BD + D^2)\zeta_{I1}^2u_{tz} + \rho_w\frac{\pi}{4}(BD + D^2)u_t\zeta_{I2} + \rho_w\frac{\pi}{4}D^2\left(\tfrac{7}{2} + 3\frac{D^2(B+D)}{(B-D)^3}\left(\log\left(\frac{B}{D}\right) - 2\frac{B-D}{B+D}\right)\right)u^2u_t/g. \tag{59}$$

Equations (58) and (59) contain ζ_{I2}. There is a contribution from the second-order incident-wave potential to ζ_{I2} in irregular sea. But, since this gives only a difference frequency effect (*cf.* Faltinsen [7 p. 169]), it does not contribute to a 3ω-effect in (58) and (59).

Figure 5 shows nondimensionalized values of $(-D_1+D_2+D_3)$ for different cross-sectional forms based on Lewis-form technique. The value is always positive. The cross-sectional form

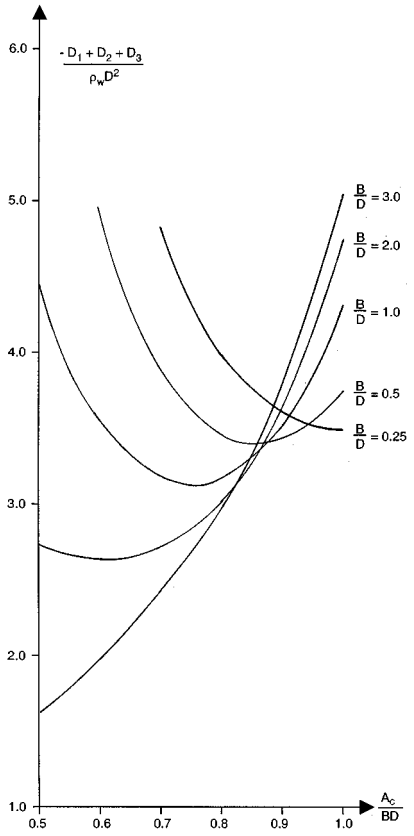

Figure 5. Horizontal force $(-D_1 + D_2 + D_3)u^2 u_t/g$ (see Equation (58)) acting on a vertical cylinder in incident irregular waves propagating in the x-direction on deep water. Cross-section is a Lewis form. D = cross-sectional length in the y-direction. B = cross-sectional length in the x-direction. A_C = cross-sectional area.

clearly influences the results. Figure 6 contains information about the two-dimensional added mass a_{11}, which is needed in Equation (58).

4. Conclusions

Third harmonic loads on a vertical cylinder in regular or irregular longcrested non-breaking waves in deep water have been analyzed. The cylinder cross-section has two symmetry axis and the waves propagate along one of the symmetry axis. The theory is a generalization of the FNV-method for circular cross-sections. A characteristic wave amplitude A is of the same order as a characteristic cross-dimension of the cylinder. This assumption is different from a conventional perturbation scheme with A as a small parameter. A characteristic wave length is large relative to a. An essential part of the analysis is a nonlinear scattering potential ψ that satisfies an inhomogeneous free-surface condition on a horizontal plane that follows the linear incident wave elevation at the cylinder axis. The forces due to ψ are reformulated into simpler expressions through the use of integral theorems and auxiliary potentials. Details have been shown for cross-sections that can be described by conformal mapping based on Lewis-form technique. Completely analytical expressions for the third harmonic loads have been derived for elliptical cross-sections. The limit of this expressions for a flat plate in cross-flow has been

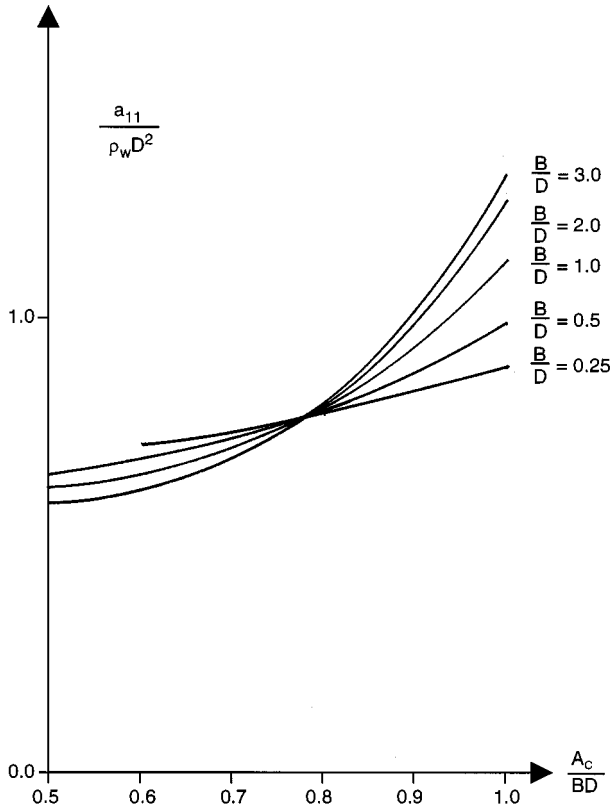

Figure 6. Two-dimensional added mass a_{11} for Lewis forms. D = cross-sectional length in the y-direction. B = cross-sectional length in the x-direction. A_c = cross-sectional area.

shown to be logarithmically singular. It was shown that the third harmonic loads are sensitive to the cross-sectional form.

References

1. O. M. Faltinsen, J. N. Newman and T. Vinje, Nonlinear wave loads on a slender vertical cylinder. *J. Fluid Mech.* 289 (1995) 179–198.
2. J. N. Newman, *Nonlinear Scattering of Long Waves by a Vertical Cylinder*. Symposium in honor of Professor Enok Palm on his 70th Birthday, The Norwegian Academy of Science and Letters, Oslo (1994) 91–102.
3. R. C. T. Rainey, A new equation for calculating wave loads on offshore structures. *J. Fluid Mech.* 204 (1989) 295–324.
4. X. Zhu, *A Higher-order Panel Method for Third-harmonic Diffraction Problems.* Ph.D. Thesis, Dept. of Ocean Engineering, MIT, Cambridge, Massachusetts, USA (1997) 124 pp.
5. S. Malenica and B. Molin, Third-harmonic wave diffraction by a vertical cylinder. *J. Fluid Mech.* 302 (1995) 203–229.
6. J. N. Newman, *Marine Hydrodynamics* Cambridge. Massachusetts: MIT Press (1977) 402 pp.
7. O. M. Faltinsen, *Sea Loads on Ships and Offshore Structures*. Cambridge: Cambridge University Press, (1990) 328 pp.
8. C. von Kerczek and E. O. Tuck, The representation of ship hulls by conformal mapping functions. *J. Ship Res.* 13 (1969) 284–298.